Article

Structure

Structure and Switch Cycle of SRβ as Ancestral Eukaryotic GTPase Associated with Secretory Membranes

Graphical Abstract

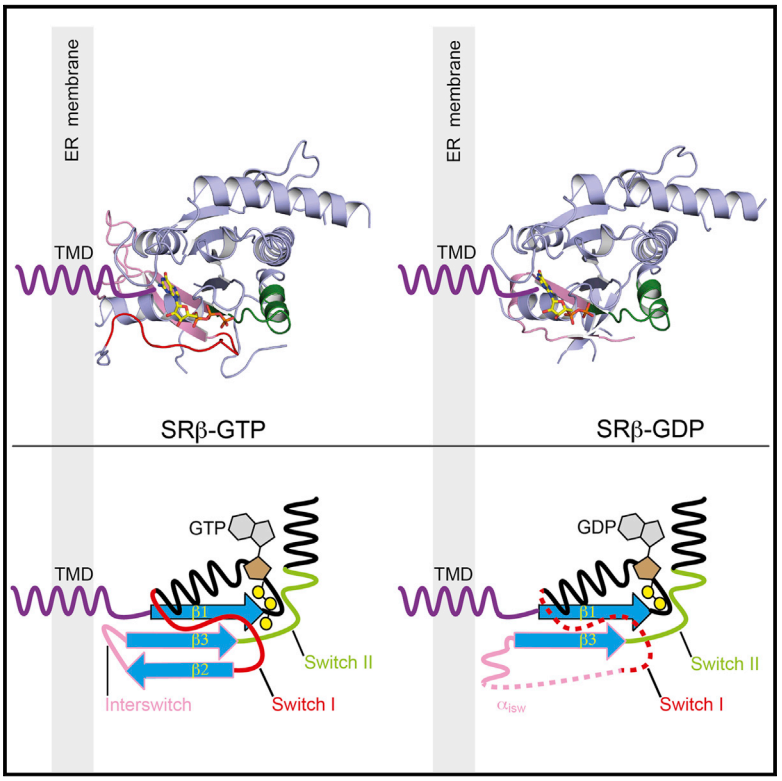

Authors

Bhalchandra Jadhav, Klemens Wild, Martin R. Pool, Irmgard Sinning

Correspondence

klemens.wild@bzh.uni-heidelberg.de (K.W.), irmi.sinning@bzh.uni-heidelberg.de (I.S.)

In Brief

Small molecular switch proteins are tracers for eukaryotic evolution. The earliest branching within this protein family involves three GTPases associated with cellular membranes. Jadhav et al. present structures and switch cycle of the SRβ subunit of the signal recognition particle receptor that targets nascent protein chains to the ER.

Highlights

- Structures of the SRβ-GTPase in its GTP- and GDP-states describe its switch cycle
- The switch cycle is unique and reveals a fixed switch II region
- A comprehensive mechanistic view on the family of Arf-like GTPases is presented
- A thermophilic fungus is used to integrate the SRβ receptor into SRP targeting

Accession Numbers

5CK3
5CK4
5CK5

Jadhav et al., 2015, Structure *23*, 1838–1847
October 6, 2015
http://dx.doi.org/10.1016/j.str.2015.07.010

CellPress

Structure
Article

Structure and Switch Cycle of SRβ as Ancestral Eukaryotic GTPase Associated with Secretory Membranes

Bhalchandra Jadhav,[1,2] Klemens Wild,[1,*] Martin R. Pool,[2] and Irmgard Sinning[1,*]
[1]Heidelberg University Biochemistry Center (BZH), Im Neuenheimer Feld 328, 69120 Heidelberg, Germany
[2]Faculty of Life Sciences, University of Manchester, Oxford Road, Manchester M13 9PT, UK
*Correspondence: klemens.wild@bzh.uni-heidelberg.de (K.W.), irmi.sinning@bzh.uni-heidelberg.de (I.S.)
http://dx.doi.org/10.1016/j.str.2015.07.010

SUMMARY

G proteins of the Ras-family of small GTPases trace the evolution of eukaryotes. The earliest branching involves the closely related Arf, Sar1, and SRβ GTPases associated with secretory membranes. SRβ is an integral membrane component of the signal recognition particle (SRP) receptor that targets ribosome-nascent chain complexes to the ER. How SRβ integrates into the regulation of SRP-dependent membrane protein biogenesis is not known. Here we show that SRβ-GTP interacts with ribosomes only in presence of SRα and present crystal structures of SRβ in complex with the SRX domain of SRα in the GTP-bound state at 3.2 Å, and of GDP- and GDP·Mg^{2+}-bound SRβ at 1.9 Å and 2.4 Å, respectively. We define the GTPase switch cycle of SRβ and identify specific differences to the Arf and Sar1 families with implications for GTPase regulation. Our data allow a better integration of SRβ into the scheme of protein targeting.

INTRODUCTION

Correct localization of proteins in the cell is the prerequisite for their proper mode of action. Proteins can be targeted to the ER in eukaryotes either in a co- or post-translational manner. In co-translational targeting, the hydrophobic N-terminal signal sequence of the client protein is recognized by the signal recognition particle (SRP) immediately on emergence from the ribosomal exit tunnel (Lingappa et al., 1984; Zopf et al., 1990). Mammalian SRP is a ribonucleoprotein complex consisting of an SRP RNA with 300 nucleotides and six proteins (SRP9/14, SRP19, SRP54, SRP68/72) (Siegel and Walter, 1988). The SRP/ribosome-nascent chain complex (RNC) is targeted to the ER membrane by GTP-dependent interaction with the SRP receptor (SR) (Connolly and Gilmore, 1989) (Figure 1A). The RNCs are then transferred to the Sec61 translocon in the ER membrane and SRP and SR subsequently dissociate on GTP hydrolysis.

The eukaryotic SR consists of the two GTPases SRα and SRβ (Tajima et al., 1986). The cytosolic SRα belongs to the SIMIBI (for SRP, MinD, BioD) class of GTPases and together with its homolog within SRP (SRP54) and FlhF (involved in flagellar biosynthesis in bacteria), these three proteins constitute the distinct subfamily of SRP GTPases (Bange and Sinning, 2013). SRP GTPases are characterized by low affinity for the nucleotides (K_D of ~10 μM) and GTPase regulation by dimerization (Gasper et al., 2009; Moser et al., 1997). SRP GTPases are multi-domain proteins. SRα consists of an N-terminal SNARE-like Longin domain (SRX domain) that is connected by a long flexible linker to the NG domain, which harbors the GTPase activity. The SRX domain is responsible for interaction with the SRβ GTPase in a GTP-dependent manner (Legate et al., 2000) (Figure 1A).

SRβ belongs to the Ras superfamily of small monomeric GTPases. Ras-like GTPases are specific for eukaryotes and serve as central regulators of cellular processes. The earliest branching event in the evolution of small GTPases is associated with the development of the secretory endomembrane systems (Jekely, 2003). This ancient family includes SRβ (targeting to the ER), Sar1 (secretion-associated and Ras-related 1) involved in ER to Golgi vesicle transport via COPII, and Arf-family proteins (ADP-ribosylation factor) responsible for retrograde and intra-Golgi trafficking via COPI vesicles. Within this family, only SRβ is permanently anchored to the membrane by an N-terminal membrane anchor (Ogg et al., 1998). Sar1 and Arf proteins are transiently attached to the membrane in their GTP-bound state on exposure of an N-terminal amphipathic helix that becomes in addition myristoylated within Arf proteins (Jekely, 2003). In contrast to the SRP GTPases, SRβ and all family members have high affinity for nucleotides (K_D in the low nanomolar range) and are not stable in the nucleotide-free state (Cherfils and Zeghouf, 2013).

Small Ras-like GTPases hardly hydrolyze GTP on their own, and GTPase-activating proteins (GAPs) and guanine-nucleotide exchange factors (GEFs) are necessary to efficiently drive their GTPase cycle (Vetter and Wittinghofer, 2001). These GTPase regulators induce extensive conformational changes within the switch I and switch II regions that shape the active sites of the GTPases. Mammalian SRβ in its soluble form (without transmembrane domain) has no detectable GTPase activity and unlike Sar1 and Arf purifies in its GTP-bound state (Legate and Andrews, 2003). RNCs were shown to interact with SRβ in a GTP-dependent manner and to stimulate GTP hydrolysis of SRβ (Legate and Andrews, 2003; Mandon et al., 2003). However, binding to ribosomes and activation requests the presence of SRα, although SRβ in its GDP-bound state can be crosslinked to ribosomes (Fulga et al., 2001). Based on its structure, the SRX domain of SRα was proposed to have a co-GAP function

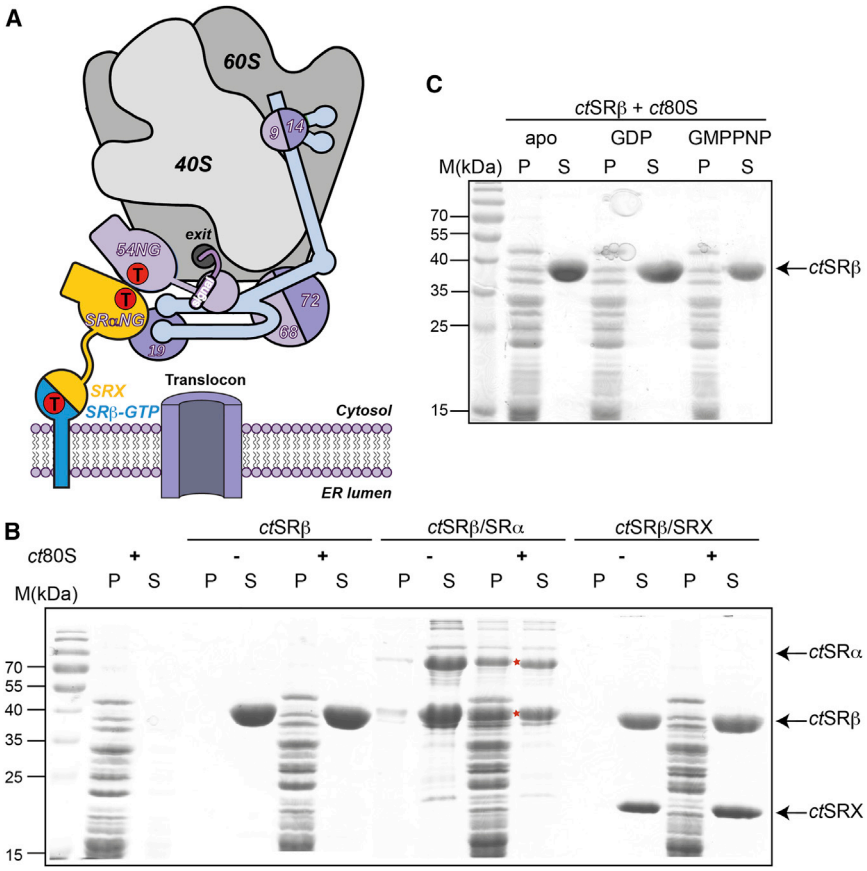

Figure 1. The SRβ-Ribosome Interaction Relies on SRα

(A) Scheme of eukaryotic SRP (light blue/purple)/SR (blue/yellow) interaction with the ribosome-nascent chain complex (gray) at the ER membrane. The SRX domain (yellow) interacts with GTP-bound SRβ (blue). T, GTP.

(B) Co-sedimentation assays for the analysis of binding efficiencies of *ct*SRβ alone or in complex with either *ct*SRα or *ct*SRX. Only *ct*SRβ bound to *ct*SRα interacts with ribosomes (respective bands are marked with red asterisks). P, pellet; S, supernatant.

(C) *Ct*SRβ does not interact with *ct*80S ribosomes. Binding efficiency of *ct*SRβ to ribosomes was tested (as in [B]) in presence of indicated nucleotides by co-sedimentation assays. Binding is not observed irrespective of the nucleotide load. See also Figure S1.

for SRβ as it stabilizes (but does not activate) SRβ in the GTP-bound state (Schlenker et al., 2006). In yeast, the GEF for SRβ could be attributed to the cytosolic loop of the β-subunit of the translocon (Helmers et al., 2003), which shares sequence similarity to the Sec7 domain of Arf-GEFs (Helmers et al., 2003) and was found to interact with the nucleotide-free state of mammalian SRβ (Schlenker, 2006).

Understanding the molecular mechanisms of GTPases relies on details of their switch cycles, which are well described for the Sar1 and Arf proteins but are lacking for SRβ. Thus, it is not clear how GTP hydrolysis in SRβ is stimulated by the SRP-SR/RNC complex and how this event links with the SRP cycle. For Sar1 and Arf, their functional specialization is defined by the unique GDP-bound state, whereas their GTP-bound state, like that of SRβ, shares the canonical features of all Ras-like GTPases. The switching of Sar1 and Arf between the soluble (GDP) and membrane-bound (GTP) states and the change in localization are mediated by a rigorous conformational change known as interswitch toggle (Kahn et al., 2006; Pasqualato et al., 2002). In this toggle mechanism, the β strands (β2 and β3) between switches I and II are shifted in register by two residues in respect to the neighboring β strand (β1) and thus allow for a front-to-back communication and the reversible displacement of the N terminus (the hasp), which is responsible for membrane anchoring. As SRβ is constantly bound to the ER membrane and deviates in the interswitch signature sequence, it is important to characterize its switch cycle, which might be different to Arf and Sar1. SRβ is the oldest member of all small GTPases branching first in eukaryotic evolution (Jekely, 2003) and hence the characterization of its switch cycle has also evolutionary significance. However, the role of SRβ as an active GTPase has remained a mystery as the GDP-bound structure of SRβ has been hitherto unavailable.

Here, we present three structures of SRβ from the thermophilic fungus *Chaetomium thermophilum* in its GDP- and GTP-bound states. SRβ features a unique switch cycle with a fixed switch II region. The comparison with Arf and Sar1 allows for a complete description of the switch cycles for the ancient family of Arf-like GTPases, from which other small GTPases seem to have evolved. The structures and biochemical data on ribosome binding also open new avenues for understanding the eukaryotic SRP cycle where SRβ adds an additional level of regulation.

RESULTS

The SRβ-Ribosome Interaction Relies on SRα

The role of SRβ in the SRP cycle is one of the big remaining questions in SRP research. A major difficulty is that functional characterization requires the context of the SRP/RNC complex and the translocon at the membrane. The interaction of the eukaryotic SR with ribosomes has been studied earlier (Bacher et al., 1999; Fulga et al., 2001; Legate and Andrews, 2003; Mandon et al., 2003). It could be shown that the linker region between the N-terminal SRX domain and the C-terminal NG domain of SRα is crucial for ribosome binding of the SR (Mandon et al., 2003). However, the influence of SRβ in different nucleotide-loaded states on ribosome binding could not be tested, as purified SRβ-GDP was not available. SRβ is notoriously insoluble in its GDP-bound state, and hence, we chose the thermophilic fungus *Chaetomium thermophilum* (*ct*) as a model system, a strategy that proved successful previously (van Noort et al.,

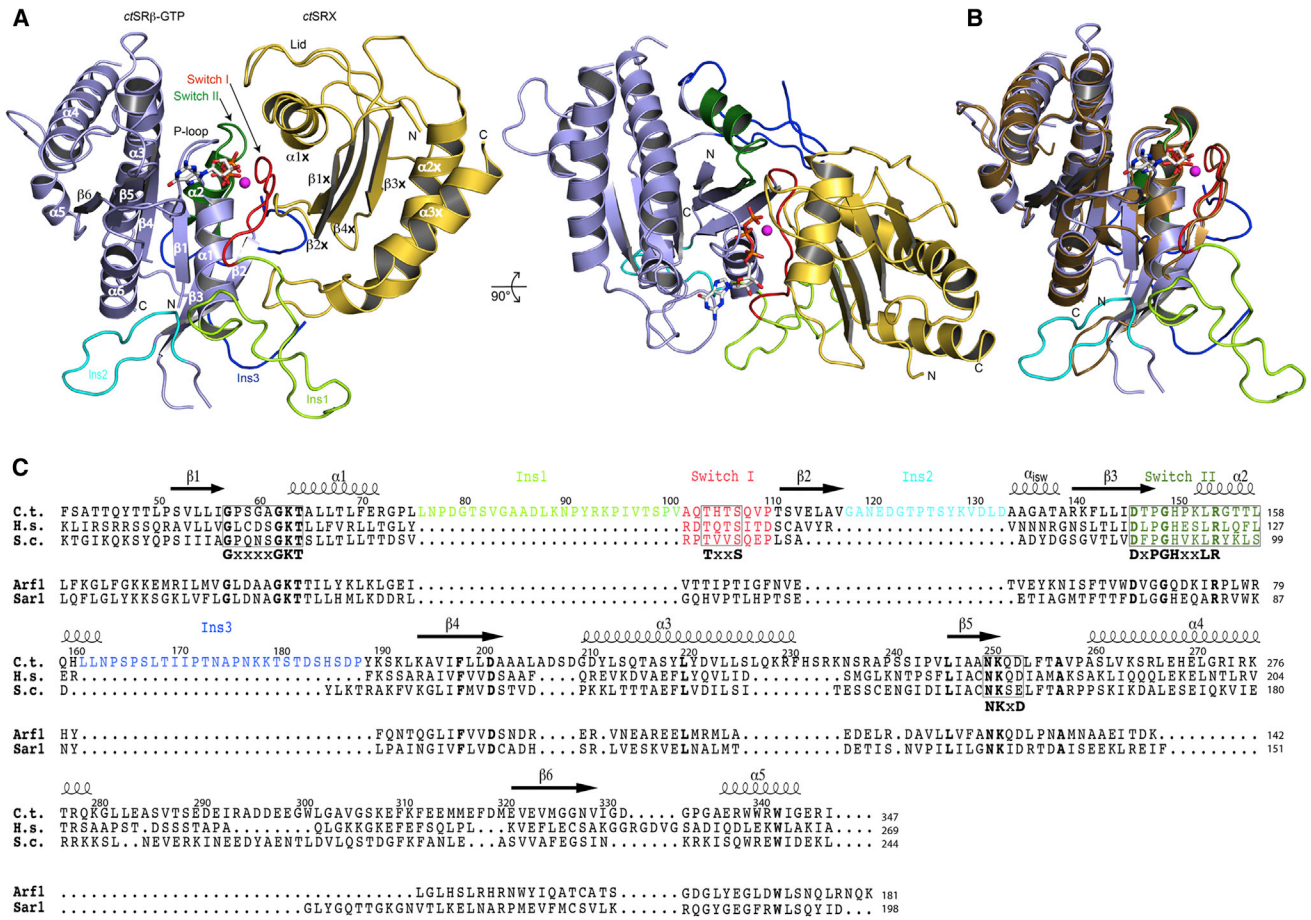

Figure 2. The Structure of *ct*SRβ-GTP/SRX

(A) Overall structure of *ct*SRβ-GTP/SRX (*ct*SRβ, blue; *ct*SRX, yellow). The switch regions and the three insertions (Ins1 to Ins3) of *ct*SRβ and all secondary structure elements are indicated. GTP is shown in sticks, Mg^{2+} is represented by a magenta sphere. The two panels are related by a 90° rotation around a horizontal axis as indicated. See also Figure S2.

(B) Superposition of the *ctSRβ-GTP* structure (colored as in [A]) with mammalian SRβ-GTP from the respective SRX complex (gold; PDB: 2fh5).

(C) Structure based sequence alignment of SRβ and human Arf1 and Sar1. Top numbering and secondary structure correspond to *ct*SRβ. The color code for *ct*SRβ is as in (B) Conserved sequence fingerprints are boxed and indicated, identical residues are in bold type. C.t., *Chaetomium thermophilum*; H.s., *Homo sapiens*; S.c., *Saccharomyces cerevisiae*.

2013). Binding of purified *ct*SR to *ct*80S ribosomes was analyzed by co-sedimentation experiments. As shown for mesophilic species, we confirm that complete *ct*SR (including *ct*SRβ-GTP) efficiently binds to *ct*80S ribosomes (Figure 1B). *Ct*SRβ alone or bound to the SRX domain of *ct*SRα was not able to bind to ribosomes, proving that neither SRβ-GTP nor SRX is necessary for ribosome interaction. However, SRβ-GDP might still bind to ribosomes, as GTPases drastically change their conformation during their switch cycle (Vetter and Wittinghofer, 2001). To analyze the influence of the nucleotide load, *ct*SRβ was converted into the nucleotide-free state and incubated with either GDP or the non-hydrolysable GTP-analog GMPPNP. In a co-sedimentation assay, we now show that *ct*SRβ does not bind to ribosomes irrespective of the nucleotide load (Figure 1C).

These results show that SRβ interacts with ribosomes only in the presence of SRα and therefore in the GTP-bound state. Stimulation of the GTPase activity of SRβ on the ribosome can therefore occur only in presence of SRα.

Structure of the *ct*SRβ-GTP/SRX Complex

As the conformation of SRβ does not directly influence ribosome binding but rather regulates the SRX interaction during the switch cycle, we set out to determine the structures of a complete set of SRβ structures in the GTP- and GDP-bound states for *Chaetomium thermophilum*. Structures of SRβ-GTP in complex with the SRX domain of SRα have already previously been reported for the mammalian (Schlenker et al., 2006) and yeast (Schwartz and Blobel, 2003) systems. These structures revealed the overall conservation of the folds regardless of low sequence homology, the regulator function of SRX by binding to the switch regions of SRβ, and described the complex as a prototype of small GTPases interacting with Longin domains (Schlenker et al., 2006). The structure of *ct*SRβ-GTP/SRX was solved by molecular replacement using the mammalian counterpart as a search model (Schlenker et al., 2006) at a resolution of 3.2 Å (Figure 2A; Table 1). The globular parts of the *ct*SRβ-GTP/SRX complex confirm the general blueprint of the domain architectures.

Table 1. Data Collection and Refinement Statistics

	*ct*SRβ-GTP/SRX	*ct*SRβ-GDP	*ct*SRβ-GDP·Mg^{2+}
Data collection			
Space group	$P2_1$	P1	$P2_1$
Cell dimensions			
a, *b*, *c* (Å)	88.3, 83.6, 90.2	34.9, 64.3, 64.9	64.1, 138.0, 64.3
α, β, γ (°)	90, 105.2, 90	86.5, 90.1, 79.6	90, 93.1, 90
Resolution (Å)	45.5–3.2 (3.3–3.2)	34.4–1.9 (2.0–1.9)	64.2–2.4 (2.5–2.4)
R_{merge} (%)	14.1 (103)	6.2 (34)	6.5 (31)
$I/\sigma I$	7.2 (1.0)	9.4 (3.0)	6.1 (2.2)
Completeness (%)	99.2 (97.7)	97.7 (96.1)	95.2 (99.5)
Redundancy	1.9 (1.9)	2.5 (2.4)	2.0 (2.0)
Refinement			
Resolution (Å)	45.5–3.2	34.4–1.9	64.2–2.4
Number of reflections	20,939 (2,029)	43,515 (4,261)	42,718 (4,465)
R_{work}/R_{free} (%)	27.6/30.0	16.5/20.4	18.6/22.3
Number of atoms	7,900	3,833	6,887
Protein	7,790	3,367	6,679
Ligand	110	56	116
Water	0	410	92
B factors (Å^2)	85.2	22.4	56.0
Rmsds			
Bond lengths (Å)	0.007	0.007	0.011
Bond angles (°)	1.21	1.05	1.41
Ramachandran (%)			
Favored	91	99	97
Disallowed	1.5	0	0.7

Values in parentheses are for the highest resolution shell. See also Figure S4.

*Ct*SRβ reveals the canonical characteristics of small Ras-like GTPases and superimposes with low root-mean-square deviations (rmsds) with its mammalian (0.80 Å for 117 Cα-atoms) (Figure 2B) and yeast (0.84 Å for 139 Cα-atoms) homologs. The long insert protruding from the SRβ core and reaching from an elongated helix α4 up to strand β6 (residues 286–310; also present in variable length in Sar1 and known as Ω loop) is retained and is partly unstructured, as previously reported. The function of this insert is unknown; however, in Sar1 it has been attributed to the regulation of COPII interactions (Huang et al., 2001). In addition to the previously described SRβ structures, *ct*SRβ contains three major insertions present in many fungi (Rosenblad et al., 2003) that cluster around the switch regions (Figure 2A) and stabilize both the *ct*SRβ-GTP/SRX interaction and the *ct*SRβ-GDP structure (see below).

On the sequence level, *ct*SRβ contains all consensus fingerprints that define the SRβ family, which like for all GTPases cluster around the nucleotide (Figure 2C). The fingerprints are GxxxxGKS/T^{64} for the P loop, TxxS^{107} within the switch I region (residues 99–110 for *C. thermophilum*), DxPGHxxLR^{154} within the switch II region (residues 146–160), and NKxD^{253} for the guanine binding pocket. Residues Thr^{64} and Ser^{107} are directly involved in magnesium coordination. The catalytic residue His^{150} is in a resting position pointing outward of the active center (Figure 3A), rendering the *ct*SRβ-GTP/SRX complex inactive (Figure S1). The histidine is tied to the backbone nitrogen of Lys^{152} within switch II and therefore it must be available in the deprotonated form. A unique feature of SRβ applies to the switch II fingerprint. The conserved fingerprint within Arf and Sar1 writes as DxGG(Q^{Arf}/H^{Sar1})xxxRxW, and this signature is the prerequisite for the family-specific interswitch toggle mechanism (Pasqualato et al., 2002). While most of the fingerprint is conserved in the SRβ family, the first glycine is replaced by the rigid proline and the terminal tryptophan is not present.

SRβ from the thermophilic fungus shares the canonical features of the SRβ family, which are slightly different from Arf and Sar1, and apart from three insertions, the *ct*SRβ-GTP structure is highly similar to the mammalian and yeast homologs.

Structural Features of the *ct*SRX Domain

SRX relates to the family of non-Syntaxin SNARE proteins (i.e. Sec22b or Ykt6p) that contain Longin domains. The Longin domain is a versatile fold involved in multiple trafficking events occurring at the endomembrane system (De Franceschi et al., 2014). The Longin domain is composed of roughly 130 residues with in general five antiparallel β strands sandwiched between three α helices (Figure 2A). While helix $\alpha1_x$ (x: in the following confers to features within SRX; $\alpha1_x$ has recently also been denoted as αp for principal (De Franceschi et al., 2014)) is accommodated in the concave surface created by the central β sheet, helices $\alpha2_x$ and $\alpha3_x$ align with the β strands on the convex side of the β sheet. Helix $\alpha1_x$ is flexibly tethered to the outer β strands. This flexibility is a characteristic feature of Longin domains, and as the helix does not completely fill the cylindrical cavity created by the β sheet, its position therefore varies in respect to the underlying β sheet as described (De Franceschi et al., 2014). Special for fungal SRX is an insertion in the linker connecting helix $\alpha1_x$ with strand $\beta3_x$, which in *ct*SRX is attached as a β hairpin and forms a lid to hold helix $\alpha1_x$ (Figure 2A).

Sequence fingerprints have not been defined for SRX, with two exceptions: a glycine (Gly^{13x}) at the tip of the $\beta1_x$-$\beta2_x$ hairpin and an asparagine (Asn^{30x}) within helix $\alpha1_x$ (Figures 3B and S2). Both residues are central to the interface with *ct*SRβ-GTP (see below). However, a closer inspection of the $\beta1_x$-$\beta2_x$ hairpin reveals that it adopts a peculiar geometry, which is shaped by hydrogen bonding within the fingerprint S/TxxG^{13x}. The conserved asparagine Asn^{30x} is part of a conserved sequence pattern (ΦNxxΦX^{1}xxΦΦX^2; Φ: hydrophobic X^{1,2}: hydrophilic), which defines the amphipathic part of helix $\alpha1_x$ involved in the interaction with *ct*SRβ-GTP. The last turn of the helix shows a rare anomaly as it is widened to a π helix, which is present also in mammalian SRX (Figure 3A).

The SRX Longin domain is a compact and versatile αβ-type protein-interaction module with diverged sequence space, but with a conserved hot spot exposed on a β hairpin and an unusual amphipathic helix flexibly linked to a concave β sheet.

The Interface of *ct*SRβ-GTP and *ct*SRX

The SRβ-GTP/SRX interface is typical for a small GTPase interacting with a regulator molecule. Even although the overall

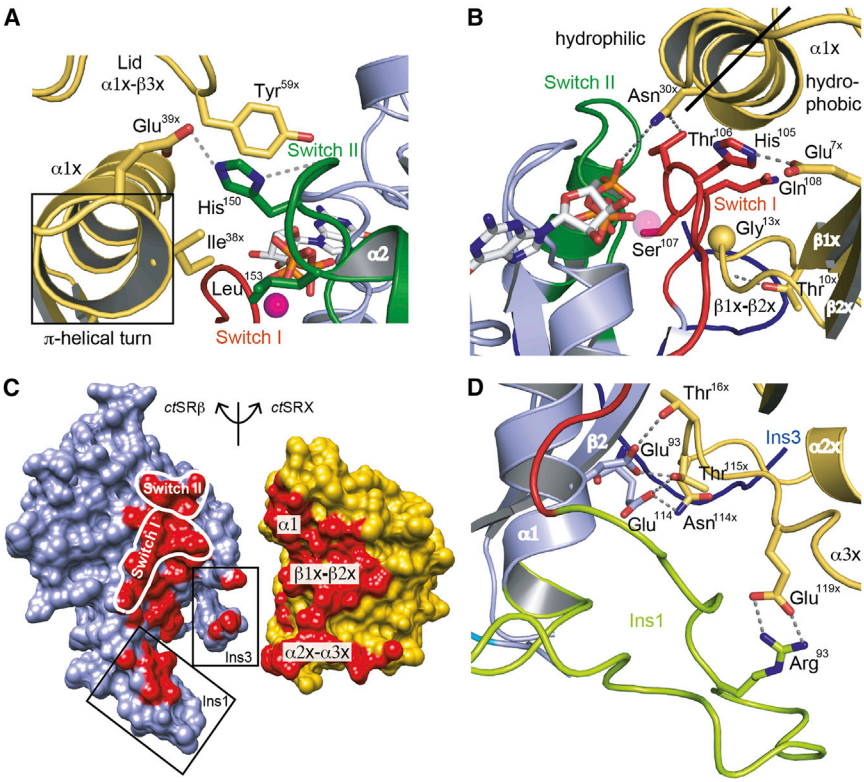

Figure 3. *Ct*SRX Stabilizes the Switch Regions of *ct*SRβ

(A) Helix $\alpha1_x$ and the lid of *ct*SRX sequester the catalytic histidine of switch II of *ct*SRβ (green). The π-helical turn of helix $\alpha1_x$ is marked by a black rectangle. A hydrophobic gate for His^{150} is formed by residues Ile^{38x} and Leu^{153}. Hydrogen bonds are shown as dashed lines. See also Figure S2.

(B) Shaping of switch I by helix $\alpha1_x$ and the $\beta1_x$-$\beta2_x$ hairpin of *ct*SRX. Important residues of the interaction are shown as sticks. A black line separates the hydrophilic and hydrophobic sides of helix $\alpha1_x$. Hydrogen bonds are shown as dashed lines.

(C) The interface of *ct*SRβ-GTP and *ct*SRX. Contact surfaces are marked in red. The areas spanned by the switch I and switch II regions are delineated by white borders and insertions are indicated by black rectangles. For visualization of the interface, the proteins are rotated in respect to the left panel of Figure 2A by ±90° around a vertical axis as indicated.

(D) Interaction of the $\alpha2_x$-$\alpha3_x$ latch of *ct*SRX with *ct*SRβ-GTP. The interswitch and insertions Ins1 and 3 frame the latch.

sequence conservation is low (Schlenker et al., 2006), the interaction including the switch regions of *ct*SRβ and a three-layered contact on *ct*SRX is highly similar in all the three homologs crystallized thus far (Figures 2A and 3C). The interface of *ct*SRβ-GTP/SRX is enlarged (1330 $Å^2$) compared with the non-thermophilic complexes (approximately 1000 $Å^2$). The increase is accomplished by two insertions (Ins1 and Ins3) confining the switch regions and probably accounting for thermostability caused by the presence of prolines, their hydrophobic nature, and increased hydrogen bonding with SRX (van Noort et al., 2013). *Ct*SRX essentially stabilizes the switch I region and thus the GTP-bound state of *ct*SRβ, and SRX does not bind to SRβ-GDP (Legate et al., 2000). The switch I region is clamped in between the $\beta1_x$-$\beta2_x$ hairpin and helix $\alpha1_x$ and so fills the extra space in the cylindrical cavity with especially two long polar residues (His^{105} and Gln^{108}) penetrating deeply into the *ct*SRX void (Figure 3B). Switch I appears hooked up by the $\beta1_x$-$\beta2_x$ hairpin, which fixes it to the bound GTP mainly by β completion involving the invariant glycine as described previously (Schlenker et al., 2006; Schwartz and Blobel, 2003). The second half of the switch I clamp is formed by helix $\alpha1_x$, which aligns with the switch over three turns ($\Phi Nxx\Phi X^1xx\Phi\Phi$) and contributes with hydrophobic and hydrophilic interactions (Figure 3B). The single invariant asparagine (Asn^{30x}) is hydrogen bonded to the main chain and side chain of threonine Thr^{106}, which also contacts the γ-phosphate of GTP.

*Ct*SRX not only contacts switch I, but also interacts with the N-terminal turn of helix α2 ($HxxL^{153}$) in the switch II region. Most importantly, the C-terminal π-helical turn of helix $\alpha1_x$ ($X^1xx\Phi\Phi X^2$) sequesters the catalytic histidine His^{150} away from the active center (Figure 3A), thus rendering the *ct*SRβ-GTP/SRX complex inactive and giving a rationale for the observed helix anomaly. The central hydrophobic residue of the turn (mostly Ile or Leu) is in close van der Waals contact with Leu^{153}. The contact forms a hydrophobic gate that prevents His^{150} to rotate (counterclockwise) in to an activated position as seen in Sar1 structures. The gate is reminiscent to elongation factor Tu (EF-Tu), where the catalytic histidine is kept in a resting position before it is activated by rRNA (Voorhees et al., 2010). In addition to the gate, His^{150} is held back by hydrogen bonding to the last residue of helix $\alpha1_x$ (X^2; Glu^{39x} in *C. thermophilum*), an interaction not described in the mammalian and yeast structures where distances are larger and hydrogen bonding is water mediated. However, in these structures the X^1 residue is hydrogen bonded to the P loop hindering a (clockwise) rotation in the active center. In yeast, this polar gate seems to functionally replace the helical anomaly in terms of histidine sequestering. In *C. thermophilum*, sequestering of the histidine is completed by an additional lid formed by the $\alpha1_x$-$\beta3_x$ loop of *ct*SRX (Figure 3A). Although electron density is weak, this lid forms a β hairpin and a tyrosine (Tyr^{59x}) at the very tip stacks on top of His^{150}. Thus, His^{150} is engaged in a cage-like environment.

The protein-protein interface is completed by an extended latch formed by the $\alpha2_x$-$\alpha3_x$ loop that grabs around the *ct*SRX β sheet and interacts with *ct*SRβ at helix α1, the interswitch region, and the *C. thermophilum*-specific insertions Ins1 and Ins3 (Figure 3D). This peripheral part of the interface is significantly extended compared with the non-thermophilic complexes because of the insertions. The overall conserved part includes the C-terminal region of helix α1 with both polar and hydrophobic interactions, and the interswitch region with main-chain and side-chain interactions.

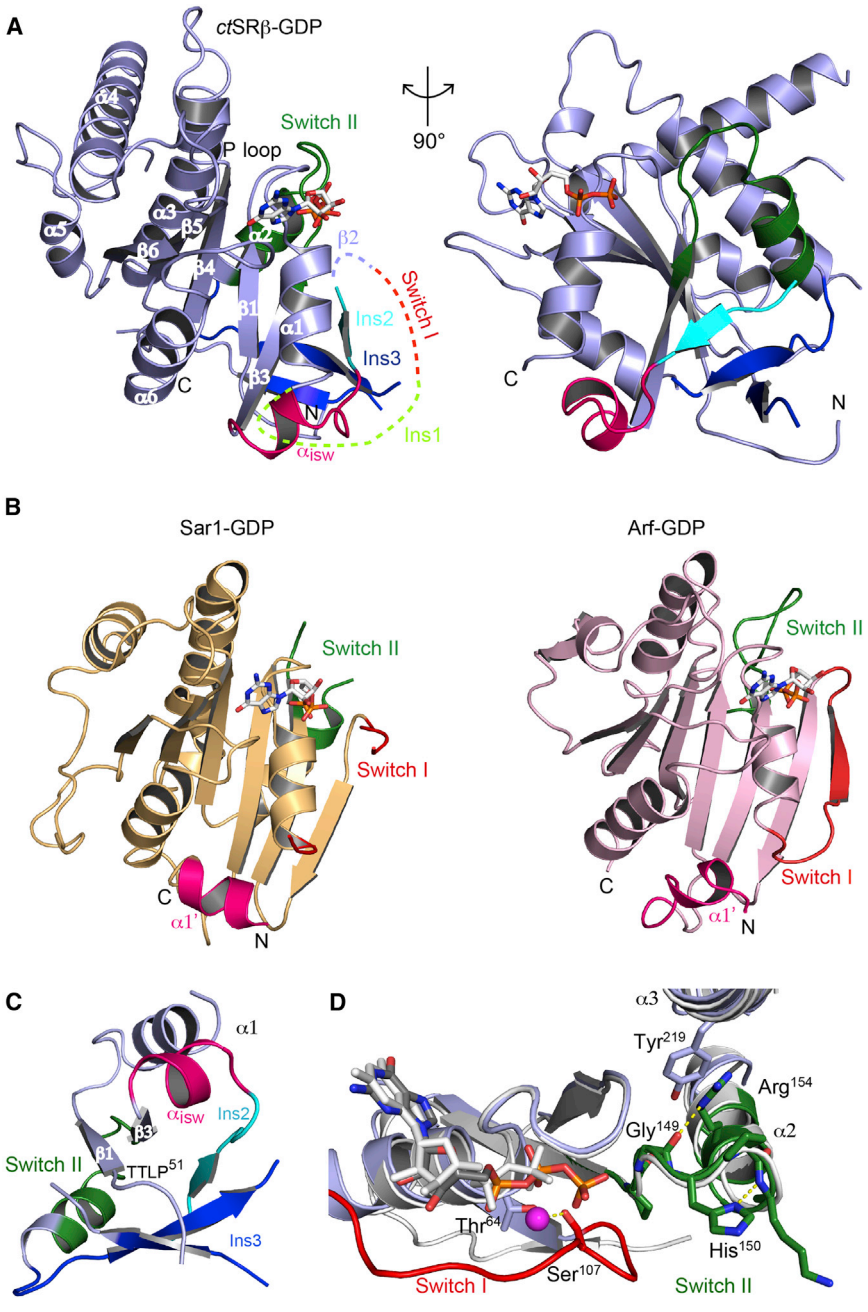

Figure 4. Structure of *ct*SRβ-GDP

(A) Overall structure of *ct*SRβ-GDP corresponding to the post-hydrolysis state. The orientation in the left panel corresponds to Figure 2B. The right panel is clockwise rotated by 90° around a vertical axis as indicated. The additional helix α_{isw} (magenta) is formed and Ins1, switch I, and strand β2 are disordered. See also Figures S3 and S5.

(B) GDP-bound structures of Sar1 (Huang et al., 2001) (brown, PDB: 1f6b) and Arf (Greasley et al., 1995) (pink, PDB: 1rrf). The switch regions are highlighted as in (A) The position of helix α1′ corresponds to helix α_{isw} in SR-GDP.

(C) The *ct*SRβ-GDP structure is stabilized by an extra β-barrel formed by Ins2 and Ins3. The barrel is incomplete (between strand β3 and the strand from Ins2). The orientation corresponds to a bottom view of the left panel in (A).

(D) Comparison of the switch regions in *ct*SRβ-GTP (blue) and *ct*SRβ-GDP (gray). Important residues in the switch regions are shown for *ct*SRβ-GTP and hydrogen bonds are given as dashed lines. Switch I is flexible in the GDP-bound state, whereas switch II does not change its conformation. A magenta sphere denotes the position of the magnesium ion.

The tight and multilayered *ct*SRβ-GTP/SRX interface is necessary to tie the switch I region onto the nucleotide and to sequester the catalytic histidine out of the active center, thereby prohibiting GTP hydrolysis.

Structure of *ct*SRβ-GDP

The crystal structure of the SRβ post-hydrolysis state could not be determined yet, as SRβ proteins expressed as soluble variants (without transmembrane helix) and in complex with SRX purify in the GTP-bound state, and attempts to exchange the nucleotide for GDP usually render the proteins unstable. However, a structure of nucleotide-free yeast SRβ was previously described revealing an unparalleled domain swap of the switch II region and involving a *cis*/*trans* isomerization of the conserved switch II proline (Schwartz et al., 2006). This aggregation-prone (circularly permutated) homodimer could be obtained only after prolonged (6 days) treatment at non-physiological pH (9.1). Small GTPases including Arf and Sar1 are commonly unstable in their nucleotide-free state in absence of a GEF (Renault et al., 2003) and switch between their GTP- and GDP-bound states (Cherfils et al., 1998; Vetter and Wittinghofer, 2001). Since the switch II proline is generally conserved in SRβ, we analyzed if *ct*SRβ undergoes homodimerization at physiological conditions and in different nucleotide loads by size-exclusion chromatography (SEC). *Ct*SRβ without SRX hydrolyzes about 25% of the bound GTP after 2 hours of incubation (Figure S3A) and is also stable in its GDP-bound state. Both GTP- and GDP-bound *ct*SRβ elute as monomers in SEC (Figure S3B for *ct*SRβ-GTP). To deplete the nucleotide, *ct*SRβ was treated with alkaline phosphatase. Nucleotide-free *ct*SRβ is soluble; however, in contrast to yeast SRβ, the removal of the nucleotide did not lead to dimerization even at a higher concentration of 40 μM (Figure S3B).

To obtain information about the GDP-bound state, we solved the structure of the stable *C. thermophilum* protein with and without magnesium at 2.4 Å and 1.9 Å resolution, respectively (Figure 4A and Figure S4). The structures are virtually identical, indicating that magnesium does not have a significant influence on the switch regions. Overall, *ct*SRβ-GDP adopts an open

conformation as also observed in the GDP-bound structures of Sar1 (Rao et al., 2006) and Arf1 (Goldberg, 1998; Greasley et al., 1995) (Figure 4B). This open conformation was found to be important for the interaction with respective GEF molecules (Goldberg, 1998; Mossessova et al., 1998). *Ct*SRβ-GDP is more similar to Sar1-GDP (sequence identity of 21%; rmsd of 1.9 Å for 131 Cα-atoms) than to Arf1-GDP (sequence identity of 18%; rmsd of 2.3 Å for 133 Cα-atoms). Most strikingly, in *ct*SRβ-GDP the switch I region together with the three major insertions completely rearrange in respect to *ct*SRβ-GTP, whereas switch II is unaffected (Figure S5).

The structural flexibility of the switch I region is typical for all small GTPases and also occurs in Sar1 and Arf. The restructuring in *ct*SRβ follows a unique mechanism influenced by all three specific insertions. The mobile elements include Ins1/switch I/Ins2/interswitch (residues 73–140) and Ins3 (residues 164–190). Most intriguingly, parts of Ins2 and Ins3 assemble in an antiparallel three-stranded β-sheet that is attached to the SRβ-core by β-barrel formation including strand β1 and the interswitch strand β3 (Figure 4C). However, the barrel is not complete and the closing sixth β strand would correspond to interswitch strand β2, which is, however, dissolved in the *ct*SRβ-GDP structure. In addition, a short α helix (α_{isw} for interswitch, residues 134–140) in the interswitch region is formed that retracts the interswitch/Ins2 region from the surface. Helix α_{isw} locates to the hydrophobic surface patch that accommodates the N-terminal amphipathic helices in Arf and Sar1 (there denoted as helix α1′). The entire Ins1 and the switch I region are disordered.

As a special case for small GTPases, the switch II region does not switch conformation between the GTP- (with SRX) and GDP-bound states (Figure 4D). The catalytic histidine (His^{150}) in the *ct*SRβ-GDP structures is flexible and points outward of the active center, being either bound to the backbone amide of Lys^{152} or disordered. Stability of switch II and the absence of the classical interswitch toggle characterizing Sar1 and Arf is manifested in three deviations in the respective signature sequences comprising strand β3 and switch II: first, within $DxPGHxxLR^{154}$ of SRβ, a proline (Pro148) replaces the first glycine; second, it includes a conserved large hydrophobic leucine (Leu153); and third, it misses the conserved tryptophan at the end. The proline residue apparently confers stability to strand β3 in contrast to the glycine, which needs to be reversibly associated with the toggling β strand and undergoes a peptide flip in the switch cycle. The proline is accommodated in a hydrophobic pocket created by the conserved leucine, likely impeding the register shift and also hindering the catalytic residue to pass the hydrophobic gate in context of SRX. The observed proline *cis/trans* isomerization concomitant with a switch swap in an artificially stabilized nucleotide-free SRβ dimer from yeast (Schwartz et al., 2006) is not observed in our *ct*SRβ-GDP structure. The invariant tryptophan in Arf and Sar1 was described to act as an aromatic wedge in the GDP-bound states to fasten switch II in a conformation incompatible with GTP binding (Pasqualato et al., 2002). This wedge pushes the switch II helix α2 (as long as it is not dissolved) away from the active site and thus detaches it from the protein core. In the GTP-bound states, the wedge is released and the tryptophan stabilizes switch II by π-cation stacking onto the conserved arginine generally conserved in the whole family. In contrast, for SRβ, the aromatic residue stacking on the arginine is supplied by the SRβ-core structure on helix α3 (Tyr^{219}) and thus the wedge is not present (Figure 4D).

The post-hydrolysis GDP-bound state of SRβ is different from Sar1 and Arf. The switch II region is fixed on the protein core and a mobile helix covers a regulatory hydrophobic surface in the interswitch region.

DISCUSSION

SRβ together with Arf and Sar1 form a distinct family of ancient eukaryotic GTPases all associated with membranes of the secretory pathway or the endomembrane system. Arf and Sar1 perform a peculiar GTPase switch cycle with an interswitch toggle mechanism allowing front-to-back communication between the nucleotide-binding site and the membrane-facing N terminus. The toggle mechanism implies conformational changes on GTP hydrolysis in both switch regions: switch I is detached from the nucleotide and switch II dissolves to follow the register shift of the interswitch (Figure 5, top). Whereas in Arf-GDP structures, switch I is detached from the nucleotide and folded onto the central β sheet to form an additional strand, in Sar1-GDP, switch I still adopts a similar (but detached) conformation as in the GTP-bound state (Huang et al., 2001; Rao et al., 2006). Switch II changes are similar in Arf and Sar1 and rely on the consensus $DxGG(Q^{Arf}/H^{Sar1})xxxRxW$.

The GTP- and GDP-bound structures of *ct*SRβ now provide a description of the switch mechanism of SRβ and a first comprehensive view on this family of ancient eukaryotic GTPases. In contrast to Arf and Sar1, SRβ is constantly anchored to the membrane by an N-terminal transmembrane helix. As SRβ branched first within this family (Jekely, 2003), it therefore might be regarded as an ancestral member and its switch mechanism to constitute a general blueprint for primordial functional specialization at the endomembrane system. As in Arf and Sar1, switch I detaches from the nucleotide in the GDP-bound state (Figure 5, bottom), a process necessary for the access of a GEF regulator to the active center. In our *ct*SRβ-GDP structures, switch I and the interswitch strand β2 are disordered; however, the structures are stabilized by the additional helix α_{isw} in the interswitch and the β-barrel formation including the insertions Ins2 and Ins3 (specific for fungi and not shown in the cartoon). The orientation of helix α_{isw} resembles the N-terminal helix α1′ in Sar1; however, there is no sequence conservation and the placement within the sequence is different. As the transmembrane helix of SRβ is permanently anchored in the ER membrane, the hydrophobic patch generated by switch I displacement is shielded by the internal amphipathic helix α_{isw}. The respective conformational changes include the displacement of strand β2 and at least for *ct*SRβ also the fixation of the C-terminal end of Ins2 (preceding α_{isw}) as strand β2′ in the β-barrel. This half-toggle of helix α_{isw} and strand β2 make the classical interswitch toggle dispensable, which would involve also strand β3 and switch II.

The structural characterization of the SRβ switch cycle leads to questions on GTPase regulation in space and time. The GAP function in GTPase activation has been attributed to the incoming SRP/RNC complex (Bacher et al., 1999) although the time point within the SRP cycle could not be defined. The EF-Tu GTPase has the same DxPGH switch II fingerprint and

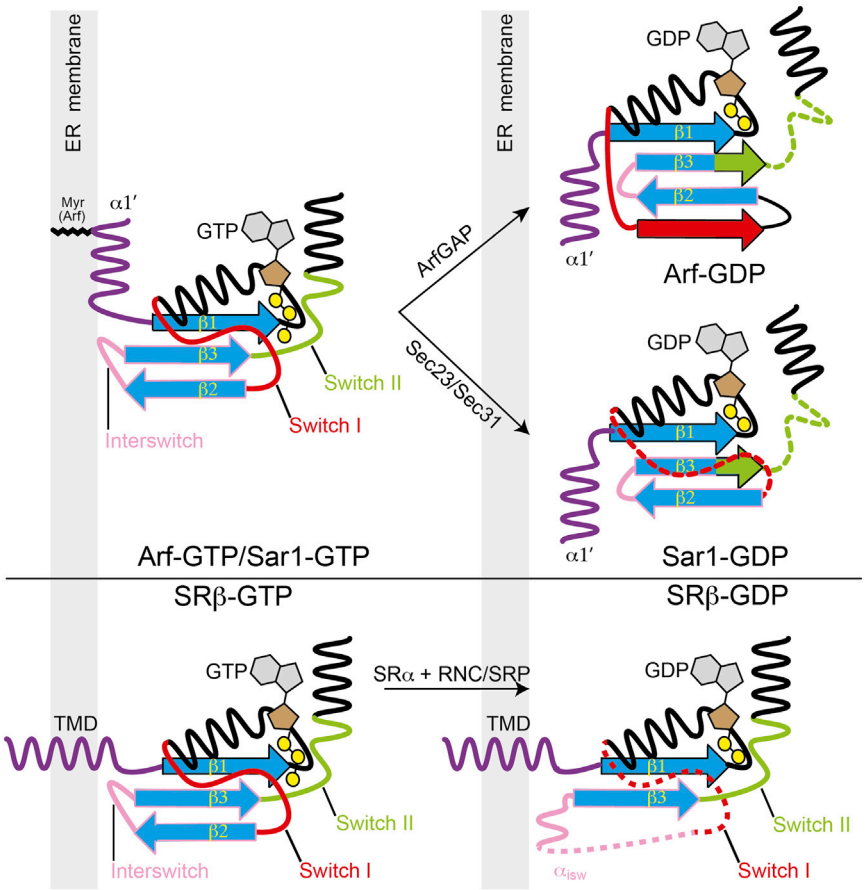

Figure 5. Distinct Switch Cycles of Small Arf-like GTPases

(Top) Schematic of structural rearrangements in the Arf and Sar1 GTPase switch cycles. The N-terminal helix α1′ forming the hasp is shown in purple. Switch I is colored red, switch II in green, and the interswitch region in pink. Dashed lines indicate flexibility. The switch mechanism involves the interswitch toggle that results in a register shift of strand β3 in respect to β1.

(Bottom) Schematic of structural rearrangements in the SRβ switch cycle. The interswitch toggle including the register shift is not present. Helix α_{isw} is formed only in SRβ-GDP corresponding to a half-toggle movement and strand β2 is disordered. SRβ-GTP corresponds to the conformation as seen in this study for *ct*SRβ-GTP/SRX.

the catalytic histidine is also sequestered away by a hydrophobic gate in the EF-Tu−GTP structure (Voorhees et al., 2010). EF-Tu is activated by rRNA (the sarcin-ricin loop) (Voorhees et al., 2010) and according to previous cryo-electron microscopy data of the SRP-SR/RNC complex (Halic et al., 2006), SRβ might be another rare case of a GTPase being activated by (SRP-)RNA. The GEF function in nucleotide exchange has been ascribed to the translocon (Helmers et al., 2003), but how this is achieved and how the membrane might orient and influence SRβ in respect to the translocon and all other compounds involved is still elusive. The profound conformational changes in switch I close to the membrane anchored N terminus as revealed by our study, however, are suggestive for re-localization events in respect to the membrane during the switch cycle as seen for Arf and Sar1. This interpretation goes in line with the discovery that an Arf-GEF-like sequence in the cytoplasmic loop of the eukaryote-specific Sec61β subunit of the translocon is responsible for the GEF function (Helmers et al., 2003). In a peptide-library approach, we could previously validate the Sec61β/SRβ interaction for the mammalian system, which exists only in the nucleotide-free state but not in the SRβ-GTP/SRX context (Schlenker, 2006). Furthermore, this study revealed interactions with an exposed loop region of Sec61α (the L6 loop) protruding from the membrane, which adds to the idea of a flexible re-orientation of SRβ-GDP in respect to the membrane. As this loop is composed of an extended β-hairpin, a β-completion with the β sheet core of SRβ-GDP could be envisaged.

What could be the role of the GTP stabilized SRβ/SRX complex in the context of the SRP cycle? Sar1 activation is known to work by a two-gear mechanism (Bi et al., 2007). In the first gear, Sar1 is stabilized in the GTP-bound state ready-for-hydrolysis by Sec23 and in cells this complex has a relatively long lifetime for a GTPase/GAP complex of about 30 s (Antonny et al., 2001; Bi et al., 2007). Similarly, the SRβ/SRX complex is a ready-for-hydrolysis state of SRβ stabilized by the SRX domain of SRα. In yeast, GTP hydrolysis in SRβ was shown not to be essential (Ogg et al., 1998), while in the mammalian system, binding of GTP to SRβ and therefore SRαβ complex formation was found to be a prerequisite for signal peptide release from SRP (Fulga et al., 2001). GTP hydrolysis in Arf and Sar1 has recently been shown to be also dispensable for the release of COPI and COPII vesicles, respectively (Adolf et al., 2013), while GTP binding per se is essential for membrane recruitment of the GTPases and coating (Adolf et al., 2013). Apparently, a primary function of small Arf-like GTPases in their GTP-bound state is therefore the targeting of the respective sorting machinery to the proper endomembrane.

The GTPase switch cycle of SRβ is unique and distinct from Arf and Sar1 as key features for the interswitch toggle are not present. SRβ acts by a half-toggle mechanism, which might be considered as a primordial switch cycle of a still membrane-bound GTPase. However, the retraction of the interswitch region next to the N-terminal membrane attachment site is conserved and distinguishes all members of this family from other small GTPases. The structural peculiarities of small Arf-like GTPases correlate with their specific roles in targeting of macromolecular complexes to secretory membranes.

EXPERIMENTAL PROCEDURES

Cloning, Expression, and Purification of ctSRβ

The gene encoding full-length *ct*SRβ (residues 1–347) was amplified from *Chaetomium thermophilum* cDNA preparation and cloned with an N-terminal

$(His)_6$-tag into the pET28d vector (Novagen) using the NcoI/NotI sites. A *ct*SRβ construct lacking the N-terminal transmembrane segment (residues 1–42) was cloned accordingly. $(His)_6$-tagged *ct*SRα and *ct*SRX (first 172 residues of *ct*SRα) were cloned accordingly. The untagged versions of the proteins were cloned in the pET21d vector (Novagen).

Purification of *ct*SRβ, *ct*SR, and *ct*SRβ-GTP/SRX

*Ct*SRβ was over-expressed in *Escherichia coli* strain BL21 (DE3) Rosetta (Novagen) at 24°C by using auto-induction medium. Cell pellets were re-suspended in a buffer consisting of 20 mM Tris-HCl (pH 8.0), 150 mM NaCl, 2 mM $MgCl_2$, 10 mM imidazol, 1 mM DTT, and 0.2% (v/v) NP40. Cells were lysed using sonication followed by passing them through the Micro fluidizer M110L (Microfluidics). The protein was purified by two-step purification involving Ni^{2+} affinity chromatography followed by SEC in a buffer consisting of 20 mM Tris-HCl (pH 8.0), 150 mM NaCl, and 5 mM $MgCl_2$. *Ct*SRβ purifies with bound GTP, which slowly hydrolyses to *ct*SRβ-GDP as a result of intrinsic hydrolysis. For purification of *ctSRβ/SRα (ctSR)*, $(His)_6$-tagged *ct*SRβ, and *ct*SRα without a tag were co-expressed in BL21 (DE3) Rosetta PlysS (Novagen) at 16°C overnight. Lysed cells were incubated with Ni^{2+} beads (Sigma) (equilibrated in lysis buffer), and the complex was first purified by Ni^{2+} affinity chromatography followed by SEC to remove unbound individual proteins. For purification of *ct*SRβ-GTP/SRX, $(His)_6$-tagged *ct*SRX and untagged *ct*SRβ were co-expressed and purification was performed as in *ct*SR.

Crystallization and Structure Determination

Purified *ct*SRβ and *ct*SRβ-GTP/SRX were concentrated to either 10 mg/ml or 20 mg/ml. Crystals of *ct*SRβ were obtained by the sitting-drop vapor-diffusion method after 5 days in buffer containing 0.2 M sodium acetate (pH 7.0) and 20% (w/v) PEG3350, whereas the crystals for SRβ-GDP·Mg^{2+} grew in 0.2 M calcium acetate, 40% (w/v) PEG600, and 0.1 M sodium cacodylate (pH 6.5). Crystals were cryo-protected in liquid nitrogen using 20%–40% (w/v) glycerol in mother liquor. Crystals of *ct*SRβ-GTP/SRX grew in 20% (w/v) PEG3350 and 0.1 M sodium citrate (pH 5.5). Data collection was performed at the European Synchrotron Radiation Facility (ESRF, Grenoble) on beamline ID23eh2. Data processing was done with the XDS package (Kabsch, 2010). The structure of *ct*SRβ-GDP was solved by molecular replacement using the Phenix suite (Afonine et al., 2010) and mammalian SRβ (PDB: 2fh5) as the search model and the structure of *ct*SRβ-GTP/SRX was solved by molecular replacement using the GDP-bound structure of *ct*SRβ and a polyalanine model of *hs*SRX as a search model. The data obtained for *ct*SRβ-GDP·Mg^{2+} showed presence of crystal twinning. The structure of *ct*SRβ-GDP·Mg^{2+} was solved using the *ct*SRβ-GDP crystal structure as a search model. Twin refinement was performed in Phenix (Afonine et al., 2010). Validation of the structure was done with COOT (Emsley et al., 2010) and MolProbity (Chen et al., 2010). PyMOL was used for preparation of structural figures. Sequence alignments were generated using ESPript3 (Robert and Gouet, 2014) and validated by structural comparison. Secondary structure assignment is according the DSSP Server (Joosten et al., 2011).

Nucleotide Load and Intrinsic GTPase Activity

The nucleotide load and intrinsic GTPase activity was analyzed by sample denaturation and high-performance liquid chromatography (HPLC) analysis. 50 μl of protein (10 mg/ml) was denatured and heat precipitated by incubation at 95°C for 5 min. Samples were centrifuged at 21,000 *g* for 10 min. The supernatant was then loaded on a Nucleosil reverse-phase column equilibrated in 10 mM Tris-HCl (pH 8.2). Nucleotides were then eluted by applying a linear salt gradient using 10 mM Tris-HCl (pH 8.2) and up to 1.5 M NaCl. The amount of nucleotide was confirmed by comparison with standard nucleotides.

Purification of *ct*80S Ribosomes and Co-Sedimentation Assays

Purification of *ct*80S ribosomes was done as described (Leidig et al., 2013). *C. thermophilum* cells were grown in a rotary shaker at 90 rpm at 55°C for 3 days and harvested with a vacuum filter. The fungal mycelia was then arranged into small ball-like structures and immediately frozen in liquid nitrogen. Frozen mycelium balls were ground to fine powder in a mortar in presence of liquid nitrogen. The powdered mycelium was then suspended in 20 mM HEPES-KOH (pH 7.5), 100 mM potassium acetate, 125 mM sucrose, 7.5 mM magnesium acetate, 1 mM DTT, and 0.5 mM PMSF and vortexed until no clumps remained in the solution. The whole suspension was subjected to centrifugation at 26,940 *g* for 15 min to remove insoluble material. For pelleting the ribosomes, the solution was overlaid on a high-salt sucrose cushion (500 mM potassium acetate, 1.5 M sucrose) prepared in lysis buffer. The material was then centrifuged at 294,000 *g* for 18 hr. The ribosome pellet was then re-suspended in 20 mM HEPES-KOH (pH 7.5), 50 mM potassium acetate, 5 mM magnesium acetate, 1 mM DTT, and 0.5 mM PMSF. The re-suspended pellet was layered on a linear sucrose gradient prepared in the re-suspension buffer and centrifuged overnight at 256,000 *g*. *Ct*80S ribosomes were separated by monitoring on a UV spectrophotometer. Purified ribosomes were stored at −80°C.

For nucleotide removal, 1 μM SRβ was incubated at 16°C overnight in 1 ml of reaction buffer (20 mM Tris-HCl pH 8.0 mM, 150 mM NaCl, 400 mM ammonium sulfate) supplemented with 35 U of calf alkaline phosphatase (NEB). A PD10 desalting column (GE Healthcare) was used to remove ammonium sulfate and nucleotides. The absence of nucleotide was confirmed by HPLC analysis as described above. For sedimentation assays, reactions using 100 pM of protein and 30 pM of *ct*80S ribosomes were assembled in 25 μl assay buffer (20 mM HEPES-KOH (pH 8.0), 2 mM MgOAc, 100 mM KOAc, 1 mM DTT) and incubated at 37°C for 20 min. The reactions were then layered on a 500 mM sucrose cushion prepared in the assay buffer and centrifuged at 264,000 *g* for 60 min. Proteins in the pellet were dissolved in sample buffer. The supernatant protein fractions were separately precipitated using 10% (w/v) trichloroacetic acid. The proteins were analyzed by SDS-PAGE and Coomassie blue staining.

ACCESSION NUMBERS

Coordinates and structure factors have been deposited in the PDB under the accession codes PDB: 5CK3, 5CK4, and 5CK5.

SUPPLEMENTAL INFORMATION

Supplemental Information includes five figures and can be found with this article online at http://dx.doi.org/10.1016/j.str.2015.07.010.

ACKNOWLEDGMENTS

Supported by Deutsche Forschungsgemeinschaft (DFG) grants SFB638 and GRK1188. We thank J. Kopp and C. Siegmann from the BZH/Cluster of Excellence:CellNetworks crystallization platform for support in protein crystallization and E. Hurt and S. Amlacher for *C. thermophilum* cDNA. Special thanks to Y. L. Ahmad, G. Stier, and R. Heinze for stimulating discussions and A. Hendricks for technical assistance. All data collection was performed at the ESRF (European Synchrotron Radiation Facility, Grenoble/France). I.S. is an investigator of the Cluster of Excellence:CellNetworks.

Received: April 30, 2015
Revised: July 15, 2015
Accepted: July 19, 2015
Published: August 20, 2015

REFERENCES

Adolf, F., Herrmann, A., Hellwig, A., Beck, R., Brugger, B., and Wieland, F.T. (2013). Scission of COPI and COPII vesicles is independent of GTP hydrolysis. Traffic *14*, 922–932.

Afonine, P.V., Mustyakimov, M., Grosse-Kunstleve, R.W., Moriarty, N.W., Langan, P., and Adams, P.D. (2010). Joint X-ray and neutron refinement with phenix.refine. Acta Crystallogr. D Biol. Crystallogr. *66*, 1153–1163.

Antonny, B., Madden, D., Hamamoto, S., Orci, L., and Schekman, R. (2001). Dynamics of the COPII coat with GTP and stable analogues. Nat. Cell Biol. *3*, 531–537.

Bacher, G., Pool, M., and Dobberstein, B. (1999). The ribosome regulates the GTPase of the beta-subunit of the signal recognition particle receptor. J. Cell Biol. *146*, 723–730.

Bange, G., and Sinning, I. (2013). SIMIBI twins in protein targeting and localization. Nat. Struct. Mol. Biol. *20*, 776–780.

Bi, X., Mancias, J.D., and Goldberg, J. (2007). Insights into COPII coat nucleation from the structure of Sec23.Sar1 complexed with the active fragment of Sec31. Dev. Cell *13*, 635–645.

Chen, V.B., Arendall, W.B., 3rd, Headd, J.J., Keedy, D.A., Immormino, R.M., Kapral, G.J., Murray, L.W., Richardson, J.S., and Richardson, D.C. (2010). MolProbity: all-atom structure validation for macromolecular crystallography. Acta Crystallogr. D Biol. Crystallogr. *66*, 12–21.

Cherfils, J., and Zeghouf, M. (2013). Regulation of small GTPases by GEFs, GAPs, and GDIs. Physiol. Rev. *93*, 269–309.

Cherfils, J., Menetrey, J., Mathieu, M., Le Bras, G., Robineau, S., Beraud-Dufour, S., Antonny, B., and Chardin, P. (1998). Structure of the Sec7 domain of the Arf exchange factor ARNO. Nature *392*, 101–105.

Connolly, T., and Gilmore, R. (1989). The signal recognition particle receptor mediates the GTP-dependent displacement of SRP from the signal sequence of the nascent polypeptide. Cell *57*, 599–610.

De Franceschi, N., Wild, K., Schlacht, A., Dacks, J.B., Sinning, I., and Filippini, F. (2014). Longin and GAF domains: structural evolution and adaptation to the subcellular trafficking machinery. Traffic *15*, 104–121.

Emsley, P., Lohkamp, B., Scott, W.G., and Cowtan, K. (2010). Features and development of Coot. Acta Crystallogr. D Biol. Crystallogr. *66*, 486–501.

Fulga, T.A., Sinning, I., Dobberstein, B., and Pool, M.R. (2001). SRbeta coordinates signal sequence release from SRP with ribosome binding to the translocon. EMBO J. *20*, 2338–2347.

Gasper, R., Meyer, S., Gotthardt, K., Sirajuddin, M., and Wittinghofer, A. (2009). It takes two to tango: regulation of G proteins by dimerization. Nat. Rev. Mol. Cell Biol. *10*, 423–429.

Goldberg, J. (1998). Structural basis for activation of ARF GTPase: mechanisms of guanine nucleotide exchange and GTP-myristoyl switching. Cell *95*, 237–248.

Greasley, S.E., Jhoti, H., Teahan, C., Solari, R., Fensome, A., Thomas, G.M., Cockcroft, S., and Bax, B. (1995). The structure of rat ADP-ribosylation factor-1 (ARF-1) complexed to GDP determined from two different crystal forms. Nat. Struct. Biol. *2*, 797–806.

Halic, M., Gartmann, M., Schlenker, O., Mielke, T., Pool, M.R., Sinning, I., and Beckmann, R. (2006). Signal recognition particle receptor exposes the ribosomal translocon binding site. Science *312*, 745–747.

Helmers, J., Schmidt, D., Glavy, J.S., Blobel, G., and Schwartz, T. (2003). The beta-subunit of the protein-conducting channel of the endoplasmic reticulum functions as the guanine nucleotide exchange factor for the beta-subunit of the signal recognition particle receptor. J. Biol. Chem. *278*, 23686–23690.

Huang, M., Weissman, J.T., Beraud-Dufour, S., Luan, P., Wang, C., Chen, W., Aridor, M., Wilson, I.A., and Balch, W.E. (2001). Crystal structure of Sar1-GDP at 1.7 A resolution and the role of the NH2 terminus in ER export. J. Cell Biol. *155*, 937–948.

Jekely, G. (2003). Small GTPases and the evolution of the eukaryotic cell. Bioessays *25*, 1129–1138.

Joosten, R.P., te Beek, T.A., Krieger, E., Hekkelman, M.L., Hooft, R.W., Schneider, R., Sander, C., and Vriend, G. (2011). A series of PDB related databases for everyday needs. Nucleic Acids Res. *39*, D411–D419.

Kabsch, W. (2010). XDS. Acta Crystallogr. D Biol. Crystallogr. *66*, 125–132.

Kahn, R.A., Cherfils, J., Elias, M., Lovering, R.C., Munro, S., and Schurmann, A. (2006). Nomenclature for the human Arf family of GTP-binding proteins: ARF, ARL, and SAR proteins. J. Cell Biol. *172*, 645–650.

Legate, K.R., and Andrews, D.W. (2003). The beta-subunit of the signal recognition particle receptor is a novel GTP-binding protein without intrinsic GTPase activity. J. Biol. Chem. *278*, 27712–27720.

Legate, K.R., Falcone, D., and Andrews, D.W. (2000). Nucleotide-dependent binding of the GTPase domain of the signal recognition particle receptor beta-subunit to the alpha-subunit. J. Biol. Chem. *275*, 27439–27446.

Leidig, C., Bange, G., Kopp, J., Amlacher, S., Aravind, A., Wickles, S., Witte, G., Hurt, E., Beckmann, R., and Sinning, I. (2013). Structural characterization of a eukaryotic chaperone–the ribosome-associated complex. Nat. Struct. Mol. Biol. *20*, 23–28.

Lingappa, V.R., Chaidez, J., Yost, C.S., and Hedgpeth, J. (1984). Determinants for protein localization: beta-lactamase signal sequence directs globin across microsomal membranes. Proc. Natl. Acad. Sci. USA *81*, 456–460.

Mandon, E.C., Jiang, Y., and Gilmore, R. (2003). Dual recognition of the ribosome and the signal recognition particle by the SRP receptor during protein targeting to the endoplasmic reticulum. J. Cell Biol. *162*, 575–585.

Moser, C., Mol, O., Goody, R.S., and Sinning, I. (1997). The signal recognition particle receptor of *Escherichia coli* (FtsY) has a nucleotide exchange factor built into the GTPase domain. Proc. Natl. Acad. Sci. USA *94*, 11339–11344.

Mossessova, E., Gulbis, J.M., and Goldberg, J. (1998). Structure of the guanine nucleotide exchange factor Sec7 domain of human arno and analysis of the interaction with ARF GTPase. Cell *92*, 415–423.

Ogg, S.C., Barz, W.P., and Walter, P. (1998). A functional GTPase domain, but not its transmembrane domain, is required for function of the SRP receptor beta-subunit. J. Cell Biol. *142*, 341–354.

Pasqualato, S., Renault, L., and Cherfils, J. (2002). Arf, Arl, Arp and Sar proteins: a family of GTP-binding proteins with a structural device for 'front-back' communication. EMBO Rep. *3*, 1035–1041.

Rao, Y., Bian, C., Yuan, C., Li, Y., Chen, L., Ye, X., Huang, Z., and Huang, M. (2006). An open conformation of switch I revealed by Sar1-GDP crystal structure at low Mg2+. Biochem. Biophys. Res. Commun. *348*, 908–915.

Renault, L., Guibert, B., and Cherfils, J. (2003). Structural snapshots of the mechanism and inhibition of a guanine nucleotide exchange factor. Nature *426*, 525–530.

Robert, X., and Gouet, P. (2014). Deciphering key features in protein structures with the new ENDscript server. Nucleic Acids Res. *42*, W320–W324.

Rosenblad, M.A., Gorodkin, J., Knudsen, B., Zwieb, C., and Samuelsson, T. (2003). SRPDB: signal recognition particle database. Nucleic Acids Res. *31*, 363–364.

Schlenker, O. (2006). Structural Characterisation of the Mammalian SRP Receptor, PhD Thesis (Germany: University of Heidelberg), urn:nbn:de:bsz:16-opus-66947.

Schlenker, O., Hendricks, A., Sinning, I., and Wild, K. (2006). The structure of the mammalian signal recognition particle (SRP) receptor as prototype for the interaction of small GTPases with Longin domains. J. Biol. Chem. *281*, 8898–8906.

Schwartz, T., and Blobel, G. (2003). Structural basis for the function of the beta subunit of the eukaryotic signal recognition particle receptor. Cell *112*, 793–803.

Schwartz, T.U., Schmidt, D., Brohawn, S.G., and Blobel, G. (2006). Homodimerization of the G protein SRbeta in the nucleotide-free state involves proline cis/trans isomerization in the switch II region. Proc. Natl. Acad. Sci. USA *103*, 6823–6828.

Siegel, V., and Walter, P. (1988). Each of the activities of signal recognition particle (SRP) is contained within a distinct domain: analysis of biochemical mutants of SRP. Cell *52*, 39–49.

Tajima, S., Lauffer, L., Rath, V.L., and Walter, P. (1986). The signal recognition particle receptor is a complex that contains two distinct polypeptide chains. J. Cell Biol. *103*, 1167–1178.

van Noort, V., Bradatsch, B., Arumugam, M., Amlacher, S., Bange, G., Creevey, C., Falk, S., Mende, D.R., Sinning, I., Hurt, E., and Bork, P. (2013). Consistent mutational paths predict eukaryotic thermostability. BMC Evol. Biol. *13*, 7.

Vetter, I.R., and Wittinghofer, A. (2001). The guanine nucleotide-binding switch in three dimensions. Science *294*, 1299–1304.

Voorhees, R.M., Schmeing, T.M., Kelley, A.C., and Ramakrishnan, V. (2010). The mechanism for activation of GTP hydrolysis on the ribosome. Science *330*, 835–838.

Zopf, D., Bernstein, H.D., Johnson, A.E., and Walter, P. (1990). The methionine-rich domain of the 54 kd protein subunit of the signal recognition particle contains an RNA binding site and can be crosslinked to a signal sequence. EMBO J. *9*, 4511–4517.